

Numerical study of the system specifications effect on the performance of a Brine/Water heat pump in combination with PhotoVoltaic Thermal solar

Mohamad Ali Jaafar¹ and Bharat Chhugani²

¹ Dualsun, Marseille (France)

² Institute for Solar Energy Research in Hamelin, Emmerthal (Germany)

Abstract

PhotoVoltaic Thermal (PVT) collectors are an exciting energy technology that produces both heat and electricity. They offer a very suitable source for brine-to-water heat pumps (HP), as PVT can be used as the direct heat source for the evaporator and additionally provide electricity for the compressor. The system combines HP and PVT to offer an efficient energy solution for the heat demands of buildings. However, there are still many uncertainties about the system design and configuration. The main goal of this paper is to study the effect of the different hydraulic configurations and the system specifications on the overall system performance. For instance, the numerical study in Strasbourg shows that a heat pump with a minimum temperature limit at the evaporator inlet of $-15\text{ }^{\circ}\text{C}$ enhances by 20 % the Seasonal Performance Factor (SPF) compared to a heat pump with a temperature limit of $-10\text{ }^{\circ}\text{C}$. However, the maximum temperature limit has a negligible impact on the system's performance. Moreover, it has also been shown that the self-consumed photovoltaic energy improves the overall system performance by 7 %.

Keywords: Photovoltaic thermal solar collectors (PVT), Heat pump (HP), energy system analysis, seasonal performance factor (SPF), numerical simulations, TRNSYS

1. Introduction

Heat Pumps (HP) coupled with Photovoltaic-Thermal (PVT) collectors are becoming more and more popular since they coproduce heat and electricity and enhance the overall system performance. Researchers and industries worldwide are studying and analyzing this combination to meet the thermal needs of buildings (Kazem et al., 2024). James et al. (2021) have concluded that PVT collectors are more efficient in combination with HP than solar thermal collectors. However, they identified future research needs relating to some limitations according to the different PVT configurations during freezing, snowfall, pressure drop and corrosion. Miglioli et al. (2023) highlighted that the integration of PVT to the evaporator side of the HP systems allows to increase the heat recovery by the heat source and then improving system performances, however, the distinction of solar and evaporator circuits would be relevant and flexible especially when a second heat source is used.

Moreover, Vaishak and Bhale (2019) have shown that the systems combining HP and PVT collectors are more energy efficient and reliable compared to other conventional and non-conventional energy resources for hot water applications. A detailed simulation study carried out by Chhugani et al. (2023) showed that PVT-heat pump systems can significantly contribute to reducing CO₂ emissions compared to fossil heating systems and represent a promising, noise-free alternative to air-source heat pumps. Furthermore, they found that combining PVT collectors with ground-coupled heat pump systems allows 35% smaller dimensioning of Borehole Heat Exchangers (BHE) with lower CO₂ emissions simultaneously.

Helbig et al. (2018) found that PVT collector designs with high heat loss coefficients (c_1 and c_2 according to ISO 9806) can work both as solar collectors and environmental heat exchangers and achieve a higher/better system efficiency with direct PVT-heat pump combinations compared to PVT collectors with lower heat loss coefficients. Jaafar et al. (2022) also showed numerically that the most influencing parameter on system performance is PVT collectors' first-order heat loss coefficient compared to other thermal coefficients.

The presented paper focuses on the effect of the different hydraulic configurations of the sink circuit and the different HP specifications on the overall performance of the system combining HP and PVT. First, it describes the system, and the numerical methodology used for this study. Then, the results are presented, comparing the different system scenarios, including different heating systems in the building and different HP specifications as maximum and minimum temperature limits at the evaporator and the compressor technology.

2. Methodology

The TRNSYS software is used for the present study. Several models (TRNSYS types) were developed and assembled to simulate HP and PVT systems, the details of the models are shown in Table 1. The PVT type used herein has been validated with experimental measurements (Chhugani, 2020). As shown in Figure 1, PVT is the single heat source of the HP that produces heat to cover the domestic hot water (DHW) and space heating (SH) needs of the building. The backup electric heater is located in the flow pipe of the heat pump. The mixing valve in front of the evaporator prevents too high temperatures from reaching the evaporator of the heat pump (set point of the mixing valve depends on the maximum temperature limit of the evaporator of the HP). The photovoltaic energy produced by PVT can be consumed directly by the HP compressor.

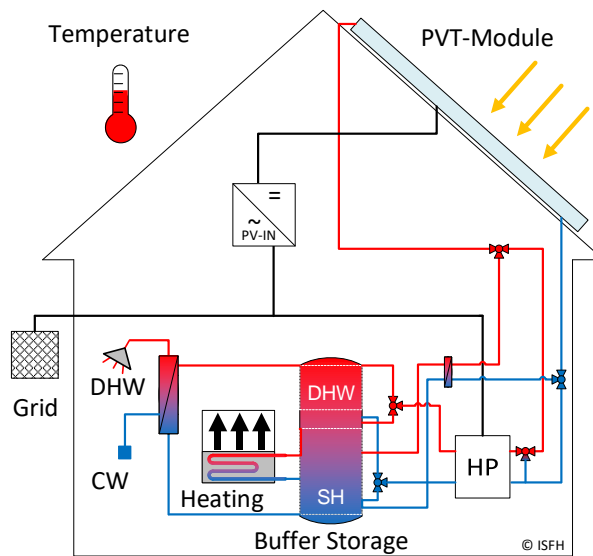


Fig. 1: The hydraulic schema of the system, including combi storage in the sink side

Tab 1: Various component models used for TRNSYS System simulations

Description	Documentation/Reference
Thermal building	TRNSYS Multi zone Building ("Multizone Building modeling with Type56 and TRNBuild," 2012)
PVT collector	Uncovered PVT (photovoltaic-thermal) collector (Stegmann et al., 2011)
Heat pump	Compressor heat pump model (Afjei and Wetter, 1997)
Thermal storage tank	Multiport thermal buffer Store tank model (Druck, 2006)
Radiator heating	Model for Radiator heating System for Buildings (Holst, 1996)

The simulation study investigates three distinct configurations of photovoltaic-thermal (PVT) systems integrated with heat pumps, as illustrated in Figure 2. All these configurations utilize PVT collectors as the sole heat source for the heat pumps, differing only in the hydraulic arrangement of the sink side. In the first configuration, a combi storage tank supplies space heating (SH) and domestic hot water (DHW) to the building, while the second configuration features two separate storage tanks, one for SH and the other for DHW. In the

third configuration, a single storage tank is used for DHW, and the SH system is directly connected to the heat pump.

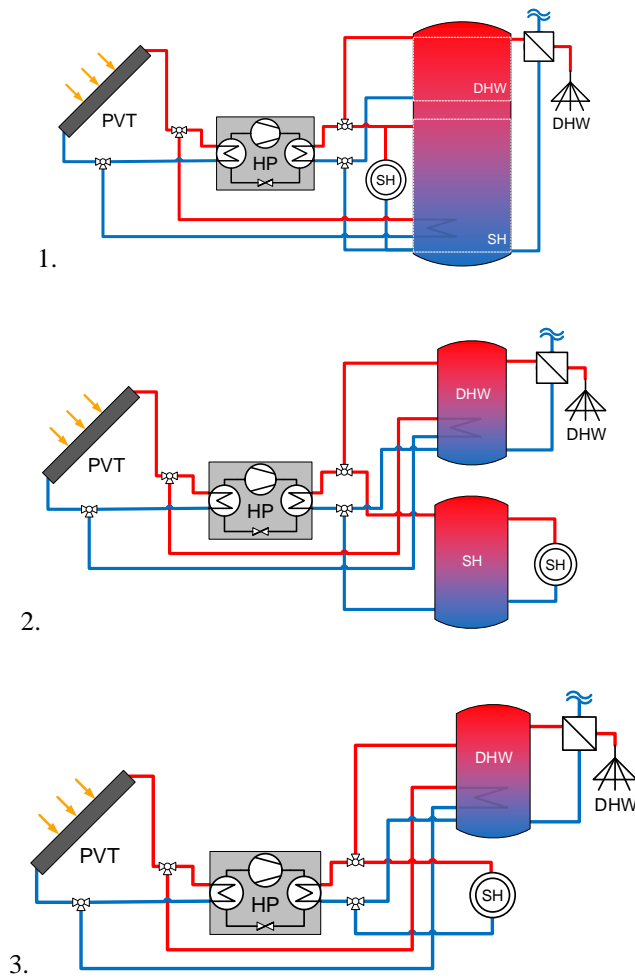


Fig. 2: The three investigated configurations of the sink side

The used building is a single-family house with a total surface of 140 m² and a space heating demand of 48 kWh/m².a. The external wall and the roof ceiling have a U-value construction of 0,28 and 0,19 W/m².K, respectively. The domestic hot water demand is 2141 kWh/a (150 L/day at 45 °C which corresponds to 3 people) and the daily domestic hot water profile is shown in Figure 3. A detailed description of the boundary conditions, load profiles, and building components (SFH45) is published in IEA Task 44 (Dott et al., 2013).

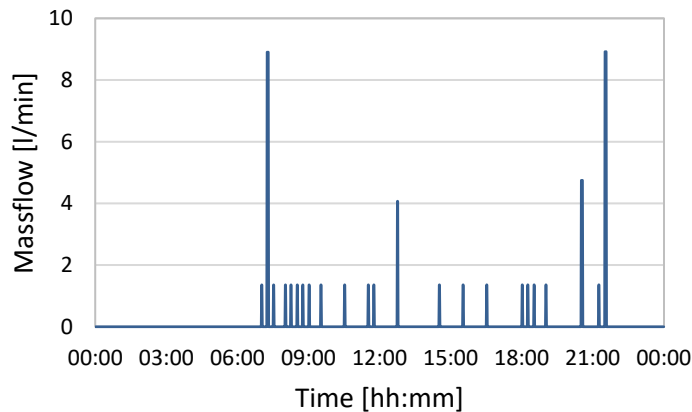


Fig. 3: Domestic hot water demand (DHW) of the building at 45°C

Additional to different configuration as shown in Figure 2, the building is also simulated with two different heating concepts: floor heating and radiator heating. Figure 4 shows the heating characteristic curves of the two different heating systems respect to flow temperature.

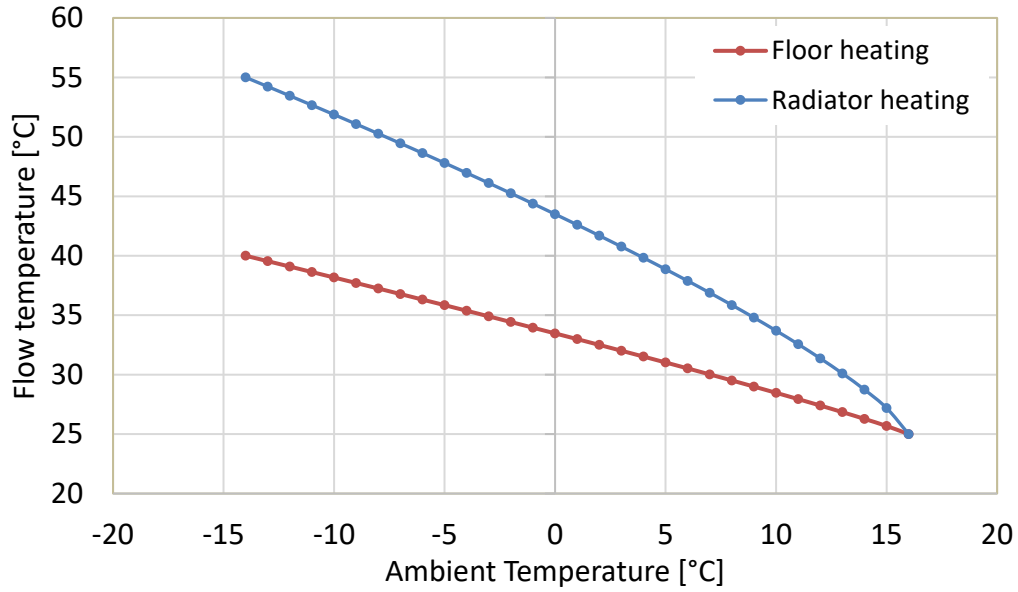


Fig. 4: Heating characteristic curves for floor and radiator heating

The simulated PVT collector, with a surface of 1.95 m² and photovoltaic peak power of 425 W, has the following thermal coefficients according to the Solar Keymark test. The parameters of the PVT collector are shown in Table 2. Additionally, in all the configurations of PVT to heat pump, the PVT collectors are regularly defrosted to account for model uncertainties below 0 °C as explained in (Chhugani, 2020).

Tab. 2: Thermal coefficients according to Solar Keymark certification (licence number 011-7S3219 P)

Coefficient	Description and [unit]	Value
$\eta_{0,b}$	Optical efficiency [-]	0,38
c1	Heat loss coefficient [W/m ² K]	37,44
c2	Temperature dependence of the heat loss coefficient [W/m ² K ²]	0
c3	Wind speed dependence heat loss coefficient [J/m ³ K]	7,31
c4	Sky temperature dependence of the heat loss coefficient [-]	0
c5	Effective thermal capacity [kJ/m ² K]	29,46
c6	Wind speed dependence conversion factor [s/m]	0,046
c7	Wind speed dependence of IR radiation exchange [W/m ² K ⁴]	0
c8	Radiation losses [W/m ² K ⁴]	0
Kd	Incidence angle modifier for diffuse solar radiation [-]	0,98

The heat pump used is an inverter whose compressor speed depends on both heat demand in the building and the heat provided by the heat source (PVT) and their temperature levels. The flow rates on the source and the sink sides are controlled to maintain a temperature difference of 5 and 3 K, respectively. The thermal power of the HP is 9.1 kW B0/W35, and the thermal output of the heat pump at different inlet temperatures and different compressor speeds is shown in below Figure 5.

During the operation of the heat pump, the mean temperature of the PVT reduces until the power equilibrium of the evaporator and PVT. A simple and robust control strategy is implemented in the numerical model. The compressor speed is adapted firstly to meet heating or domestic hot water demand as well as to avoid cut-off of the compressor due to very high temperatures or very low temperatures on the evaporator side. The adaption is done according to the compressor envelope, as shown in Figure 6. The distinction is also made between

space heating and domestic hot water loading since the heat pump must provide heat at different temperature levels.

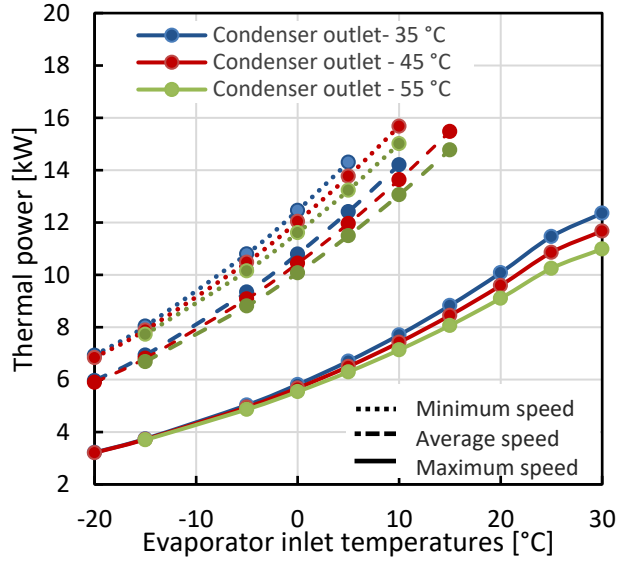


Fig. 5: Thermal output (y-axis) at different evaporator inlet temperatures (x-axis) for condenser outlet temperatures for the minimum, average and maximum compressor speed.

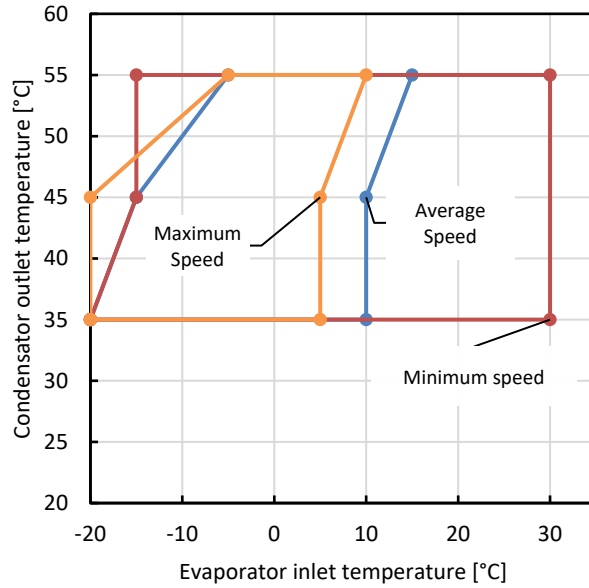


Fig. 6: Compressor envelope of the brine-water heat pump with different compressor speeds

For each system scenario, the thermal Seasonal Performance Factor (before storage) is defined as the ratio between the produced thermal energy and the consumed electric energy by the system. For a whole year of system operation, it can be calculated following this equation (Eq. 1):

$$SPF = \frac{\int (\dot{Q}_{HP} + \dot{Q}_{backup} + \dot{Q}_{PVT,Defrosting}) dt}{\int (\dot{E}_{HP} + \dot{E}_{backup} + \dot{E}_{pump,defrosting}) dt} \quad Eq. 1$$

\dot{Q} stands for the supplied heat and \dot{E} stands for the electric consumption of each component.

As an additional system indicator, the SPF_{Grid} considering the self-consumed photovoltaic energy by the heat pump is calculated following this equation (Eq. 2):

$$SPF_{Grid} = \frac{\int (\dot{Q}_{HP} + \dot{Q}_{backup} + \dot{Q}_{PVT,Defrosting}) dt}{\int (\dot{E}_{HP} + \dot{E}_{backup} + \dot{E}_{pump,defrosting} - \dot{E}_{PV_{el_self}}) dt} \quad Eq. 2$$

The difference between the indicators shows the enhancement in the system performance due to the photovoltaic energy produced by the PVT and at the time if the HP is running, it consumes this photovoltaic electricity. Otherwise, this energy is consumed by other electric equipment in the building (without household electricity) and rest of the electricity is sent to the grid. In all cases, this photovoltaic energy is a very important source of CO₂ emissions and money saver for the building owner.

All the simulations are performed with 10 PVT and a 9,1 kW (B0/W35) HP. The five studied parameters are detailed in the following:

- The sink circuit hydraulic configuration as shown in Figure 2: combi storage (560L used for both DHW and SH), double storages (one of 200L for DHW and another of 300L for SH) or only one storage for DHW (200L, the SH is connected directly to the condenser of the HP).
- The compressor technology: inverter or fixed-speed.
- Minimum and maximum temperature limits of the HP evaporator. When the temperature at the PVT outlet is lower than the minimum temperature limit, the HP is not allowed to provide heat to the system and the electric backup is activated. When the temperature at the PVT outlet is higher than the maximum temperature limit, the flow rate in the PVT circuit is reduced thanks to the mixing valve so that the temperature at the inlet of the evaporator does not exceed this maximum limit.
- The heating system used to distribute heat in the building is floor heating or water radiators (heating curves are illustrated in Figure 4).

3. Results

According to the above-described methodology, the obtained results of both SPF and SPF_{Grid} are provided in the following table:

Tab. 3: The obtained results according to the different system scenarios

Scenario	Hydraulic configuration	Compressor technology	T _{eva_min}	T _{eva_max}	Heating system	SPF	SPF _{Grid}
1	Combi storage	Inverter	-15 °C	+25 °C	Floor heating	3,6	3,87
2	Double storages	Inverter	-15 °C	+25 °C	Floor heating	3,55	3,8
3	One storage for DHW	Inverter	-15 °C	+25 °C	Floor heating	3,33	3,56
4	Combi storage	Inverter	-10 °C	+25 °C	Floor heating	2,8	2,99
5	Combi storage	Inverter	-5 °C	+25 °C	Floor heating	1,9	2,1
6	Combi storage	Inverter	-15 °C	+10 °C	Floor heating	3,55	3,79
7	Combi storage	Inverter	-10 °C	+20 °C	Floor heating	2,75	2,94
8	Combi storage	Inverter	-15 °C	+ 25 °C	Radiators	3,33	3,53
9	Combi storage	ON/OFF	-10 °C	+ 25 °C	Floor heating	2,56	2,73

The results of the influencing parameters are shown in Figure 7. These results show that no matter what the system specifications are, the SPF_{Grid} (orange markers) are, according to all the studied scenarios, higher by almost 7% than the thermal SPF (blue markers). This shows that the photovoltaic energy produced by the PVT enhances the system's overall performance, saving both money and CO₂ emissions. It is green electricity available by PVT at free to use and the smart control strategies can be applied here in the future to enhance more self-consumption, which increases the SPF_{Grid}. The rest of the photovoltaic energy can feed other electric equipment in the building, otherwise it can be sent back to the electrical grid. In all cases, it brings benefits to the building and the environment saving both money and CO₂ emissions. The following subsections discuss only thermal SPF according to each parameter studied.

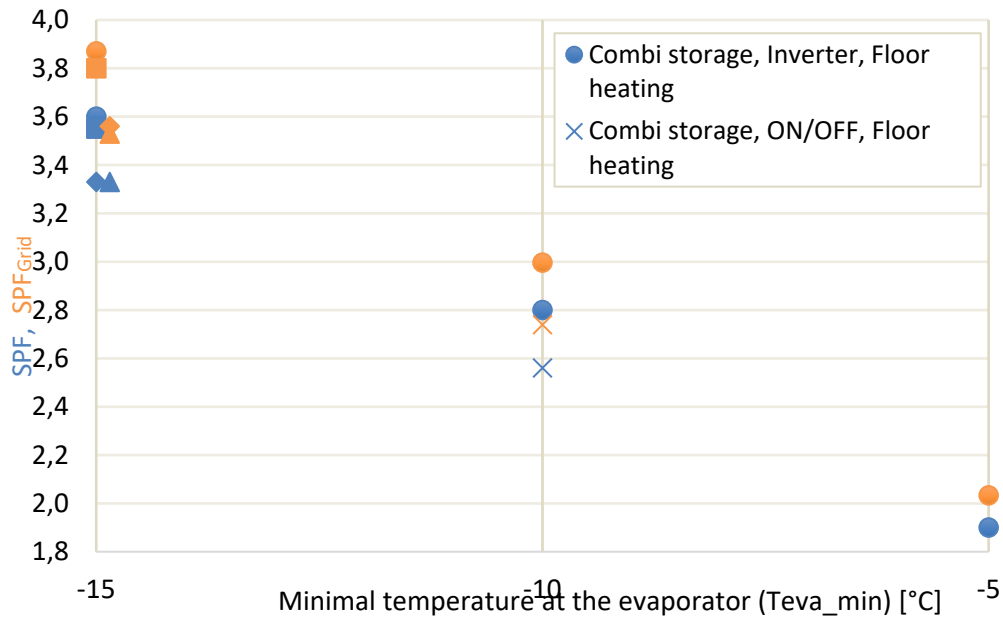


Fig. 7: The obtained results of the system performances SPF (blue markers) and SPF_{Grid} (orange markers)

3.1. Maximum temperature limit of the evaporator

When the PVT is directly connected to the evaporator of the HP, special attention must be given to the high temperatures that can be provided by the PVT, especially during summer and sunny times. When the temperature produced by the PVT exceeds the maximum temperature limit of the evaporator, which is a characteristic of the HP depending on both the used refrigerant inside the HP and the compressor operating map, the flow rate from the PVT is derived by the mixing valve so that the evaporator is protected. Although it is a critical topic in protecting HP operations, the results show that the maximum temperature limit on the evaporator side does not influence the overall system performance. The comparison between scenarios 1 (SPF = 3,6) and 6 (SPF = 3,55) and between scenarios 4 (SPF = 2,8) and 7 (SPF = 2,75) shows that the SPF is not really impacted (the system is more performant by less than 2% with higher maximum limits) when the maximum limit is decreased for both cases. It is worth mentioning that scenario 6 with +10°C represents the lowest maximum limit existing in the market of brine/water HP. The obtained result is normal for two reasons. The first is that it is a low-temperature application in which the HP does not require high temperatures to operate and provide heat in the building. The second is that the recorded average temperature at the outlet of the PVT is -1 °C, showing that temperatures that are too high are rarely observed, only during the summer season when there is no space heating demand in the building. Since the maximum temperature limit does not influence the system performance, the results according to it are not shown in Figure 7.

3.2. Minimum temperature limit of the evaporator

As for the maximum temperature limit, the minimum one is also a characteristic of the HP. However, the results show that it is a crucial parameter on the system performance: the SPF is significantly deteriorating when the minimum temperature limit increases. According to the obtained results, the system performance decreases by 22% when the minimum temperature limit passes from -15 °C (SPF scenario 1 = 3,6) to -10 °C (SPF scenario 4 = 2,8) and by 32% when it passes from -10 °C (SPF scenario 4 = 2,8) to -5 °C (SPF scenario 5 = 1,9). The impact of the minimum temperature limit can be clearly seen in Figure 7 where the horizontal axis shows the minimum temperature limit in the curve. For the exact system specifications, circle markers follow a decreasing curve when this limit increases. It has an average effect on system performance since the HP cannot run anymore, and the electric backup is activated when the temperature at the PVT outlet is lower than the minimum temperature limit of the evaporator. The minimum temperature limit is reached quicker when it is higher for the same heat source (same number of the same PVT) and the same heat demand. One must give special attention to this parameter when coupling HP with PVT.

3.3. Compressor technology (fixed or variable speed)

A variable speed, also called inverter, heat pump can adjust the speed of its compressor according to what happens in its surroundings: the heat source and the heat sink. It has many operation points according to the temperature levels in the evaporator and the condenser as well as to the heat demand. This technology is useful to save the overall electricity consumed and ensures a longer lifetime for the system with smooth and progressive HP start and stop. Numerical simulations have been performed to study the impact of this technology compared to the classic one: constant speed, also called ON/OFF, heat pump, which no matter what is happening in its surroundings, has only one compressor speed. The comparison between the scenarios 4 and 9 in Table 3 for a minimum temperature limit of $-10\text{ }^{\circ}\text{C}$ of the evaporator shows that the inverter HP (SPF scenario 4 = 2,8) is more performant than a constant speed one (SPF scenario 9 = 2,56). This difference of almost 9% is also observed in Figure 7 for a minimum temperature limit of $-10\text{ }^{\circ}\text{C}$ for the evaporator between the blue circle and the blue cross. The difference obtained is not as great as expected. This can be explained by the hydraulic configuration of the sink circuit, including a storage tank, which softens the impact of ON/OFF technology since the excess heat produced by the HP is stored for another time.

3.4. Hydraulic configuration of the sink circuit

Three different hydraulic configurations of the sink circuit between the heating system and the condenser of the HP are studied herein. All the configurations include storage for the domestic hot water. The SPF of configurations, including storage for the space heating (combi storage or double storage), are almost equal: 3,6 and 3,55 according to scenarios 1 and 2 in Table 3 and circle and square blue markers in Figure 7. The slight difference can be explained by the fact that the combi storage has less heat losses than the double storages overall the year since its surface is lower than the total surface of the double storages.

However, the configuration including only one storage for the DHW while the space heating is directly connected to the condenser of the HP has the lowest SPF (scenario 3 = 3,33 in Table 3, with the diamond blue marker in Figure 7) compared to the others. The deterioration of almost 7% in the SPF is explained by the fact that the space heating system has less thermal inertia with no heat storage, which causes many start and stop losses of the HP. At the beginning of each cycle, the compressor starts for a few seconds before the condenser produces heat in the space heating. These frequent starting cycles make the system consume electricity without being useful for longer than the configurations, including storage for the SH.

3.5. Heating system in the building

The impact of the heating system was studied for the same building. As expected, the obtained results show that the use of water radiators instead of the floor heating deteriorates by almost 7% the SPF of the system. The scenario 9 with water radiators has an SPF of 3,33 (blue triangle in Figure 7) lower than the SPF of the scenario 1 (blue circle in Figure 7) which is 3,6. This is obvious since the water radiators require higher temperature level to the HP condenser than the floor heating to distribute the same amount of heat in the building. The higher the gap between the evaporation and condensation temperatures, the less the HP is performant (see Figure 4).

4. Conclusions

The present paper investigated the different system specifications on the performance of the energy system combining brine/water heat pump with photovoltaic thermal solar collectors. The condenser of the heat pump produces heat to satisfy both domestic hot water and space heating of the building. The photovoltaic thermal solar collectors constitute the single heat source of the heat pump evaporator thanks to the back-side integrated heat exchanger and can feed the compressor with electricity thanks to the front-side photovoltaic cells. The concept is simple and performant, the photovoltaic thermal solar collectors use both the sun and the ambient air to extract heat from environment feeding the evaporator of the heat pump.

The numerical study presented herein was done using the TRNSYS software by combining the TYPES of the system components. For the same solar installation, the study investigated the system specifications, such as the heat sink hydraulic configuration and the heating system as well as the heat pump specifications, such as the compressor technology and both minimum and maximum temperature limits of the evaporator.

The simulations were performed for a well-insulated single-family house of 140 m^2 in Strasbourg (France).

The energy system is composed of 10 photovoltaic thermal solar collectors connected directly to the primary circuit of a 9.1 kW B0/W35 brine/water heat pump. Both thermal and grid seasonal performance factors have been estimated for each simulated scenario.

The results have shown the following:

- The photovoltaic energy produced by the solar collectors improves the system performance by 7 % no matter the other system specifications are.
- With space heating storage in the secondary circuit, the inverter compressor heat pump performs 9 % better than a fixed-speed heat pump. We think that this enhancement would be higher when the space heating system is directly connected to the heat pump condenser.
- The maximum temperature limit of the evaporator has no impact on the system performance. However, the minimum temperature limit is critical on the system performance. The thermal SPF of a heat pump with a $-15\text{ }^{\circ}\text{C}$ of a minimum temperature of the evaporator is 3,6 while the SPF of a $-10\text{ }^{\circ}\text{C}$ and $-5\text{ }^{\circ}\text{C}$ are 2,8 and 1,9, respectively.
- The presence of any type of water storage between the heat pump and the heating system in the building ensures a better system performance than the sink configuration without any storage.
- A floor heating system performs better than water radiators since the required flow temperature is lower.

5. References

Afjei, T., Wetter, M., 1997. Type 401, TRNSYS Compressor heat pump including frost and cycle losses, version 1.1.

Chhugani, B., 2020. Model Validation and Performance Assessment of Unglazed Photovoltaic-Thermal Collectors with Heat Pump Systems, in: Proceedings of the ISES EuroSun 2020 Conference – 13th International Conference on Solar Energy for Buildings and Industry. Presented at the EuroSun 2020, International Solar Energy Society, Online, pp. 1–12. <https://doi.org/10.18086/eurosun.2020.05.13>

Chhugani, B., Pärtsch, P., Helmling, S., Giovannetti, F., 2023. Comparison of PVT - heat pump systems with reference systems for the energy supply of a single-family house. *Solar Energy Advances* 3, 100031. <https://doi.org/10.1016/j.seja.2022.100031>

Dott, R., Haller, M.Y., Ruschenburg, J., Ochs, F., Bony, J., n.d. A technical report of subtask C Report C1 Part B. Part B.

Druck, Harald, 2006. TRNSYS Type 340, MULTIPORT Store - Model. Stratified fluid storage tank with four internal heat exchangers, ten connections for direct charge and discharge and an internal electrical heater.

Helbig, S., Kirchner, M., Giovannetti, F., Lampe, C., Littwin, M., Kastner, O., 2018. PVT-Kollektoren als bisolare Wärmepumpenquelle – Ein Simulationsvergleich zwischen Polysun und TRNSYS.

Holst, 1996. TRNSYS Models for Radiator Heating Systems.

Jaafar, M.A., Chhugani, B., Brottier, L., 2022. Numerical Study of the Effect of Hybrid Solar Collectors on the Performances of the System Combining PVT With Heat Pumps, in: Proceedings of EuroSun 2022 - ISES and IEA SHC International Conference on Solar Energy for Buildings and Industry. Presented at the EuroSun 2022 - ISES and IEA SHC International Conference on Solar Energy for Buildings and Industry, International Solar Energy Society, Kassel, Germany, pp. 1–8. <https://doi.org/10.18086/eurosun.2022.08.06>

James, A., Mohanraj, M., Srinivas, M., Jayaraj, S., 2021. Thermal analysis of heat pump systems using photovoltaic-thermal collectors: a review. *J Therm Anal Calorim* 144, 1–39. <https://doi.org/10.1007/s10973-020-09431-2>

Kazem, H.A., Chaichan, M.T., Al-Waeli, A.H.A., Sopian, K., 2024. A systematic review of photovoltaic/thermal applications in heat pumps systems. *Solar Energy* 269, 112299. <https://doi.org/10.1016/j.solener.2023.112299>

Miglioli, A., Aste, N., Del Pero, C., Leonforte, F., 2023. Photovoltaic-thermal solar-assisted heat pump systems for building applications: Integration and design methods. *Energy and Built Environment* 4, 39–56. <https://doi.org/10.1016/j.enbenv.2021.07.002>

Multizone Building modeling with Type56 and TRNBuild, 2012.

Stegmann, M., Bertram, E., Rockendorf, G., 2011. Model of an Unglazed Photovoltaic Thermal Collector Based on Standard Test Procedures, in: *Proceedings of the ISES Solar World Congress 2011*. Presented at the ISES Solar World Congress 2011, International Solar Energy Society, Kassel, Germany, pp. 1–9. <https://doi.org/10.18086/swc.2011.19.30>

Vaishak, S., Bhale, P.V., 2019. Photovoltaic/thermal-solar assisted heat pump system: Current status and future prospects. *Solar Energy* 189, 268–284. <https://doi.org/10.1016/j.solener.2019.07.051>